The Effect of Non–Insulin-dependent Diabetes Mellitus and Obesity on Glucose Transport and Phosphorylation in Skeletal Muscle

David E. Kelley,* Mark A. Mintun,§ Simon C. Watkins,‡ Jean-Aime Simoneau,‖ Fayegh Jadali,§ Alan Fredrickson,‡ Janice Beattie,* and Remy Thériault‖

*Departments of *Medicine, ‡Cell Biology and Physiology, and ‡Radiology, University of Pittsburgh, Pittsburgh, Pennsylvania 15261; §Department of Veterans Affairs, Pittsburgh, Pennsylvania 15240; and ‖Physical Activity Sciences Laboratory, Laval University, Ste-Foy, Quebec, Canada*

Abstract

Defects of glucose transport and phosphorylation may underlie insulin resistance in obesity and non–insulin-dependent diabetes mellitus (NIDDM). To test this hypothesis, dynamic imaging of ^{18}F-2-deoxy-glucose uptake into midthigh muscle was performed using positron emission tomography during basal and insulin-stimulated conditions (40 mU/m^2 per min), in eight lean nondiabetic, eight obese nondiabetic, and eight obese subjects with NIDDM. In additional studies, vastus lateralis muscle was obtained by percutaneous biopsy during basal and insulin-stimulated conditions for assay of hexokinase and citrate synthase, and for immunohistochemical labeling of Glut 4. Quantitative confocal laser scanning microscopy was used to ascertain Glut 4 at the sarcolemma as an index of insulin-regulated translocation. In lean individuals, insulin stimulated a 10-fold increase of 2-deoxy-2[^{18}F]fluoro-D-glucose (FDG) clearance into muscle and significant increases in the rate constants for inward transport and phosphorylation of FDG. In obese individuals, the rate constant for inward transport of glucose was not increased by insulin infusion and did not differ from values in NIDDM. Insulin stimulation of the rate constant for glucose phosphorylation was similar in obese and lean subjects but reduced in NIDDM. Insulin increased by nearly twofold the number and area of sites labeling for Glut 4 at the sarcolemma in lean volunteers, but in obese and NIDDM subjects translocation of Glut 4 was attenuated. Activities of skeletal muscle HK I and II were similar in lean, obese and NIDDM subjects. These in vivo and ex vivo assessments indicate that impaired glucose transport plays a key role in insulin resistance of NIDDM and obesity and that an additional impairment of glucose phosphorylation is evident in the insulin resistance of NIDDM. (*J. Clin. Invest.* 1996. 97:2705–2713.) Key words: glucose transport • insulin resistance • skeletal muscle • positron emission tomography • Glut 4

Introduction

Glucose transport is a rate-limiting step for insulin-stimulated glucose utilization in skeletal muscle (1, 2), and is a potentially important site of insulin resistance in obesity and non–insulin-dependent diabetes mellitus (NIDDM)[1] (3). The structure and expression of the insulin-regulated glucose transporter, Glut 4, is normal in most individuals with obesity or NIDDM (4–7), but insulin-regulated translocation of Glut 4 was not assessed and this is essential for functional competence of Glut 4 (8, 9). With regard to the initial phosphorylation of glucose, the primary structure of hexokinase II is normal in most patients with NIDDM (10–12) and total HK activity in skeletal muscle appears to be normal in NIDDM (13). It has been difficult to ascertain in vivo rates of insulin-stimulated glucose transport and phosphorylation in human studies. The "glucose clamp" method (14), determines insulin sensitivity but does not separate glucose transport and phosphorylation from subsequent steps of metabolism. Indirect evidence of impaired glucose transport in NIDDM was obtained by Butler et al. (15), using a combination of isotope and indirect calorimetry determinations of insulin regulated glucose oxidation. Impairment of insulin-stimulated glycogen synthesis in NIDDM (16), does not exclude a proximal impairment of glucose transport or phosphorylation, particularly since decreased skeletal muscle [G-6-P] has also been found in NIDDM (17). Bonnadonna et al., using forearm balance with isotope methods have examined the kinetics of insulin-stimulated glucose transport in muscle (18), and find impairment of glucose transport (19) and phosphorylation (20) in NIDDM.

Insulin-regulated glucose transport and phosphorylation have been extensively studied in vitro. Frequently, 2-deoxyglucose is used for this purpose because it is minimally and slowly metabolized after phosphorylation (21). Positron emission tomography (PET) imaging of regional uptake of a short-lived tracer, 2-deoxy-2[^{18}F]fluoro-D-glucose (FDG), may provide the technology for analogous in vivo assessments of glucose transport and phosphorylation (22–24). After bolus injection of FDG, serial PET imaging can define uptake curves from which kinetic rate constants for transport and phosphorylation can be determined (24, 25). In healthy volunteers, skeletal muscle insulin sensitivity determined by PET imaging is strongly correlated with systemic or forearm uptake of glucose (26–28). However, the rate constants for glucose transport and phosphorylation were not presented in these studies. Mossberg et al. validated the application of dynamic PET imaging for studying kinetics of insulin action in rabbit skeletal muscle (29). In human studies with PET imaging of insulin regulated

Address correspondence to David E. Kelley, M.D., Associate Professor of Medicine, University of Pittsburgh School of Medicine, Division of Endocrinology and Metabolism, E-1140 Biomedical Science Tower, Pittsburgh, PA 15261. Phone: 412-648-9770; FAX: 412-648-7047; E-mail: kelley@novell1.dept-med.pitt.edu

Received for publication 14 November 1995 and accepted in revised form 26 February 1996.

The Journal of Clinical Investigation
Volume 97, Number 12, June 1996, 2705–2713

1. *Abbreviations used in this paper:* FDG, 2-deoxy-2[^{18}F]fluoro-D-glucose; NIDDM, non–insulin-dependent diabetes mellitus.

glucose metabolism in skeletal muscle, Selberg et al. found that the insulin resistance of cirrhosis was due to reduced inward transport of glucose without abnormalities of glucose phosphorylation (30). Conversely, in PET studies of patients with muscular dystrophy, a reduction in the rate constant for glucose phosphorylation was found and this correlated with the length of mutation in DNA encoding for a protein kinase (31). These limited applications of PET imaging suggest it has potential for the study of insulin regulated glucose transport and phosphorylation in muscle.

The current study was undertaken to test the hypothesis that impaired glucose transport and phosphorylation within skeletal muscle contribute to insulin resistance in obesity and NIDDM. Dynamic PET imaging of mid-thigh muscle uptake of FDG was performed during basal and insulin-stimulated conditions in lean and obese nondiabetic and obese NIDDM volunteers. Rate constants for glucose transport and phosphorylation were derived from the time course of skeletal muscle FDG activity after bolus injection. In separate studies, percutaneous muscle biopsies were obtained during basal and insulin-stimulated conditions for assessment of hexokinase activity and to examine translocation of Glut 4 to the sarcolemma. In biopsy sections, Glut 4 was immunolabeled and Glut 4 at the sarcolemma was determined using quantitative confocal laser scanning microscopy. The findings of these studies indicate that impaired glucose transport and phosphorylation, together with impaired Glut 4 translocation, are important components of insulin resistance in NIDDM and obesity.

Methods

Subjects. Lean and obese nondiabetic and obese NIDDM subjects were recruited by advertisement. Clinical characteristics of the subjects are shown in Table I. Obese nondiabetic and NIDDM subjects had similar body mass index. Groups were well-matched for age and gender distribution. Lean and obese nondiabetic subjects had normal glucose tolerance, while NIDDM subjects had moderate fasting hyperglycemia. The NIDDM subjects treated with sulfonylureas ($n = 5$) had this medication withdrawn at least two weeks prior to studies; the remaining NIDDM subjects ($n = 3$) were treated by diet alone. The mean known duration of NIDDM was 3±1 years. There were significant group differences in plasma triglyceride ($P < 0.01$), with the highest values in NIDDM subjects (0.68±0.05, 1.18±0.17, and 1.98±0.29 mmol/liter; L, O, and NIDDM respectively). Lean and obese nondiabetic subjects had higher HDL cholesterol than did NIDDM subjects (1.22±0.10, 1.15±0.12 and 0.88±0.05 mmol/liter). Plasma cholesterol was not significantly different across groups (4.63±0.22, 5.30±0.30 and 5.75±0.48 mmol/liter; L, O, and NIDDM respectively).

Volunteers had a medical examination before participation. In nondiabetic subjects, this included a 2-h 75 gram oral glucose tolerance test and those with impaired glucose tolerance were excluded (32). Volunteers were free of serious medical conditions (other than NIDDM) and had normal values for hematologic, renal, thyroid, and hepatic function. NIDDM volunteers with diabetic complications of symptomatic neuropathy, ≥ 1+ proteinuria (by dipstick measurement), > mild background retinopathy, known coronary or peripheral vascular disease, or insulin treatment were excluded. The protocol was approved by the University of Pittsburgh Institutional Review Board and subjects gave written, informed consent prior to their participation.

Table I. Clinical Characteristics of Research Volunteers

	Lean (4M/4F)	Obese (4M/4F)	NIDDM (5M/3F)
Age (yr)	45±3	45±3	53±3
Wt (kg)	69±4	98±6*	105±5*
BMI (kg/m^2)	23.3±0.7	31.5±1.2*	34.1±1.4*
FPG (mg/dl)	90±2	91±2	180±27**
HbA1c	5.4±0.3	5.3±0.2	8.2±0.7**

*$P < 0.05$ vs. lean; **$P < 0.05$ vs. lean and obese.

Study design. Research volunteers underwent two insulin infusion studies. The first study (study 1) involved percutaneous muscle biopsies during basal and insulin-stimulated conditions. Muscle was obtained for immunohistochemical and high resolution microscopy studies of Glut 4 and for assay of hexokinase and citrate synthase activity. Systemic insulin sensitivity was measured during these euglycemic insulin infusion studies. The second insulin infusion study (study 2) involved PET studies of skeletal muscle uptake of ^{18}FDG during basal and insulin-stimulated conditions. The studies were separated by approximately 2–4 wk for each subject. Two lean subjects underwent PET imaging but did not have muscle biopsy studies, two additional lean volunteers were recruited for the muscle biopsy studies and did not undergo PET imaging.

For all studies, subjects were admitted to the University of Pittsburgh General Clinical Research Center on the morning of a study, having been instructed to fast overnight. Additional instructions were to refrain from exercise on the day before these studies and to maintain a carbohydrate intake of at least 200 grams daily for 3 d preceding admission. A catheter was placed in an antecubital vein for insulin infusion and another catheter was placed in the retrograde direction in a dorsal vein of the hand for blood sampling. A heating pad was used to warm this hand to arterialize samples. During study 1, a primed (20 μCi), continuous (0.20 μCi/min) infusion of 3-[^{3}H]glucose was started ~ 90 min before insulin infusion, so that systemic rates of glucose utilization could be determined during the final 30 min of a 3-h insulin infusion (40 mU/m^2 per min). After 60 min of bed rest and before insulin infusion, a percutaneous biopsy of the vastus lateralis muscle was obtained as previously described (33). A portion of this sample was placed in 2% paraformaldehyde for 1 h, then cryoprotected in 30% sucrose overnight before processing for microscopy studies and the remainder of the biopsy sample was immediately frozen in liquid N_2 for latter assay of hexokinase and citrate synthase activity. After starting insulin infusion, a variable rate 20% dextrose infusion was used to maintain euglycemia; in NIDDM subjects plasma glucose was allowed to decrease to 90 mg/dl. 3-[^{3}H]Glucose was added to the D_{20} infusion in order to maintain stable plasma glucose specific activity (34). At 180 min of insulin infusion, a second percutaneous muscle biopsy was obtained. In three of the NIDDM subjects, it was necessary to extend the clamp to maintain at least 60 min of euglycemia before the second muscle biopsy. During the 30 min before muscle biopsy, blood was sampled at 10-min intervals for plasma insulin and glucose radioactivity.

PET imaging studies of ^{18}FDG uptake into muscle were performed at the University of Pittsburgh Positron Emission Tomography Center. Infusion and blood sampling catheters were placed in the same manner as described above. A PET study was performed during basal conditions. Subjects were positioned in the ECAT 951R/31 PET scanner (Siemens Medical Systems), so that mid-thigh corresponded to the midpoint of the scanner's 10.8 cm axial field-of-view. A 20-min transmission scan was collected using enclosed rotating rods of ^{68}Ge/^{68}Ga, to measure individual attenuation coefficients which were applied during reconstruction of images for quantitative mapping of radioactivity. Dynamic PET imaging took place over 90 min, beginning with intravenous injection of 4 mCi of ^{18}FDG; synthesis of 2-deoxy-2[^{18}F]fluoro-D-glucose (FDG) was accomplished via a modification of the Hamcher method (35). Dynamic PET imaging was comprised of four frames at 30-s intervals, four frames at 1-min intervals, four frames at 2-min intervals, four frames at 5-min intervals, and four

frames at 10-min intervals. Blood sampling for plasma ^{18}FDG radioactivity began simultaneously with PET scanning at the same intervals. Blood was centrifuged and radioactivity in 100 μl plasma was counted using a Packard Canberra well counter. Cross calibration of the well counter to the PET scanner into absolute μCi/cc was performed. At completion of the PET scan during basal conditions, subjects were removed from the PET scanner and an insulin infusion (40 mU/m^2 per min) was started. Euglycemia was maintained and at 180 min of insulin infusion, subjects were returned to the PET scanner for a second imaging study of ^{18}FDG uptake into mid-thigh, repeating the procedures described above. Insulin and dextrose infusions were continued during PET imaging.

PET image and data analysis. Each of the 20 frames which comprised the dynamic PET scanning consisted of 31 contiguous 3-mm-thickness cross-sectional images of both mid-thigh regions, so that ~ 10 cm of mid-thigh length was scanned. Scanning was done in the conventional 2-D mode over a 10.8 axial field-of-view, with inherent resolution of 7 mm full with half-maximum (FWHM) in the axial dimension and 6 mm FWHM in the transaxial plane. PET images were reconstructed with in-plane image resolution of 8 mm FWHM. A region of interest (ROI) is placed within lateral and medial quadriceps on PET images of both legs and applied to the 25 inner slices on each of the 20 PET frames, so that time activity curves were constructed with data from ~ 1,000 mid-thigh images of muscle FDG radioactivity. Radioactivity enclosed by the ROIs on a PET frame was integrated and expressed as mean counts per pixel. After decay correction of each mean tissue activity value, the result was multiplied by the calibration factor and expressed as μCi/cc.

A three compartment model (24) for FDG tissue activity in skeletal muscle was used to derive rate constants of ^{18}FDG uptake, transport and phosphorylation; this model was originally developed by Sokoloff et al. (25), for brain and applied later to other organs (28–30). According to this model, the first order rate constants in the three-compartment model, K_1 (ml/min per gram) and k_2 (min^{-1}) refer to the inward and outward transport of FDG. The rate constants k_3 (min^{-1}) and k_4 (min^{-1}) refer to the phosphorylation of FDG and dephosphorylation of FDG-6-P. Arterialized blood time-activity curves were used as an input function. The model assumes that ^{18}FDG is administered in trace amounts, glucose metabolism in tissues is in steady state, the transport of FDG and FDG-6-P between compartments have first-order kinetics, and arterial plasma glucose concentration is constant. In addition, the model requires that compartments are homogenous and that the arterial plasma concentration can be used to approximate the mean capillary concentration. In this work it was further assumed that k_4, was negligible over the duration of these studies. The influx constant (K) of FDG, which reflects clearance of FDG from blood to tissue, is calculated from the relationship of the individual rate constants according to the equation: $K = (K_1k_3)/(k_2+k_3)$. Rates of glucose utilization of glucose can be estimated from FDG uptake as the product of K and arterial glucose, with a factor termed the "lumped constant" (LC) as the denominator. The LC is the ratio of analog (FDG) to true glucose utilization (22, 36). Nuutila et al. estimated that LC = 1 for skeletal muscle in healthy volunteers during euglycemic insulin-stimulated condition (26).

Immunohistochemical labeling of Glut 4 and microscopic analyses. Skeletal muscle was fixed for 1 h in 2% paraformaldehyde in phosphate buffered saline pH 7.4 (PBS), washed in PBS, then cryoprotected in 30% sucrose overnight. Muscle was mounted on filter paper and immediately frozen in CryoKwik (Fisher Scientific). 5-μm sections were cut using a Micron cryostat and mounted on Superfrost slides (Fisher). After removal from the cryostat chamber, slides were washed twice in PBS, and three times in PBS containing 0.5% BSA and 0.15% glycine (Buffer A). To block nonspecific binding of the anti-Glut 4 antibody, sections were incubated for 1 h in 5% normal goat serum in Buffer A. Subsequently, sections were incubated for 1 h in primary antibody (a rabbit polyclonal directed to Glut 4); the bindings characteristics of this antibody to Glut 4 and Glut 1, and its use in confocal laser microscopy studies of Glut 4 have been previously described (37). Sections were washed three times in Buffer A, incubated in Biotinylated anti–rabbit secondary antibody for 1 h then followed by incubation in streptavidin Cy3 tertiary marker, washed a further three times in Buffer A, three washes in PBS and mounted in Gelvatol (Monsanto). Observation was made with a Molecular Dynamics Multiprobe 2001 confocal laser microscope. Random regions of sectioned muscle were scanned for each paired specimen (basal and insulin-stimulated) using a Nikon 60× objective, 1024 × 1024 pixels, 512 illuminating laser line, 535 primary dichroic, 570 barrier filter. Images were collected under exactly the same conditions of laser brightness. Images were stored as 8 bit TIFF images, allowing 256 grey scale values. Image processing was performed using Optimas, a PC based image processing package. The periphery of all fibers within the image field were delimited, and the number, size, and intensity of labeling (as reflected by grey scale value above background) was measured and the perimeter of all fibers was also measured. The number of Glut 4 label sites are calculated per unit length of sarcolemma (μm), and the units for area Glut 4 label sites are μm^2. Analysis was done "blinded" as to the clinical status of a subject.

Enzyme activity in skeletal muscle. At biopsy, a portion of the muscle sample was frozen in liquid N_2 and maintained at −80°C. Samples were shipped on dry ice to Laval University (JAS) for analysis of hexokinase (HK; EC 2.7.1.1) and citrate synthase (CS; EC 4.1.3.7). Muscle was homogenized in an ice-cold extracting medium (0.1 M Na-K-Phosphate, 2 mM EDTA, pH = 7.2) and stirred on ice during 15 min with a small magnetic bar with 1% Triton X-100. Activities of HK and CS were determined spectrophotometrically, using previously described methods (38). In addition to total activity of HK, supernatant was heated at 45°C for one hour and then re-assayed for HK activity; because of its heat lability, this procedure removes ~ 95% of HK II activity (39). Residual HK activity in heated samples was calculated as HK I activity.

Substrate and hormone assays. Plasma glucose was measured using a YSI Glucose Analyzer (Yellow Springs, OH). Plasma glucose radioactivity was determined with liquid scintillation spectometry after de-proteinizing plasma and evaporating supernatant to dryness to remove tritiated water, as previously described (40). Rates of glucose appearance and utilization were calculated using the equations of Finegood (34). Plasma insulin was measured by radioimmunoassay.

Statistics. Data are expressed as mean±SEM. Analysis of variance was used to examine for significant differences across group (L, O, and NIDDM) and time (basal vs. insulin-stimulated). A Bonferoni corrected value for $P < 0.05$ was considered significant.

Results

Insulin sensitivity. During fasting conditions in Study 1, plasma insulin was lower in lean than obese or NIDDM subjects ($P < 0.01$), but not significantly different in obese and NIDDM subjects (40±4, 74±13, and 145±36 pmol/liter). During insulin infusion, plasma insulin was similar in obese and NIDDM subjects (571±29 and 587±47 pmol/liter, respectively) and lower in lean subjects (476±32 pmol/liter, $P < 0.05$); euglycemia was achieved in NIDDM subjects and maintained in nondiabetic subjects (89±1, 90±1, and 89±1 mg/dl, in L, O, and NIDDM subjects respectively). There were significant group differences ($P < 0.001$), in rates of insulin-stimulated systemic utilization of glucose (M). In lean, obese and NIDDM subjects respectively, the values for M were: 9.6±0.9, 5.4±0.4, and 2.8±0.3 mg/kg per min. There were also significant group differences for insulin-stimulated rates of glucose oxidation (3.1±0.2, 2.5±0.3, and 1.5±0.3 mg/kg per min, $P < 0.05$), and nonoxidative glucose metabolism (6.5±0.8, 3.0±0.4, and 1.3±0.4 mg/kg per min, $P < 0.001$; L,O and NIDDM respectively). During the final 30 min of insulin infusion, hepatic glu-

cose production was completely suppressed in lean and obese nondiabetic subjects (0.10±0.1 and −0.04±0.2 mg/kg per min), but not in subjects with NIDDM (0.96±0.24 mg/kg per min). During insulin infusions of study 2, which involved the PET imaging studies, euglycemia was also maintained in all subjects. Steady-state plasma insulin concentrations were lower in lean than either obese or NIDDM subjects (462±30, 561±40, and 610±39 pmol, $P < 0.01$), and these values were not significantly different from study 1. Systemic glucose utilization was not measured isotopically during PET imaging; however, rates of exogenous glucose infusion during these studies were strongly correlated with the respective individual rates during study 1 ($r^2 = 0.87$, $P < 0.001$), and there was a similar pattern of group differences; (L > 0 > NIDDM; $P < 0.01$).

PET studies. Arterial and mid-thigh muscle tissue ^{18}FDG radioactivity over 20 frames of dynamic PET scan are demonstrated in Fig. 1. During basal conditions, clearance of FDG into mid-thigh muscle (K), was equivalent in lean and obese nondiabetic subjects and reduced in NIDDM subjects ($P <$ 0.01), as shown in Fig. 2 *A*. K increased during insulin infusion in all groups ($P < 0.01$), and there were significant group differences in these values ($P < 0.001$). In lean subjects, insulin-

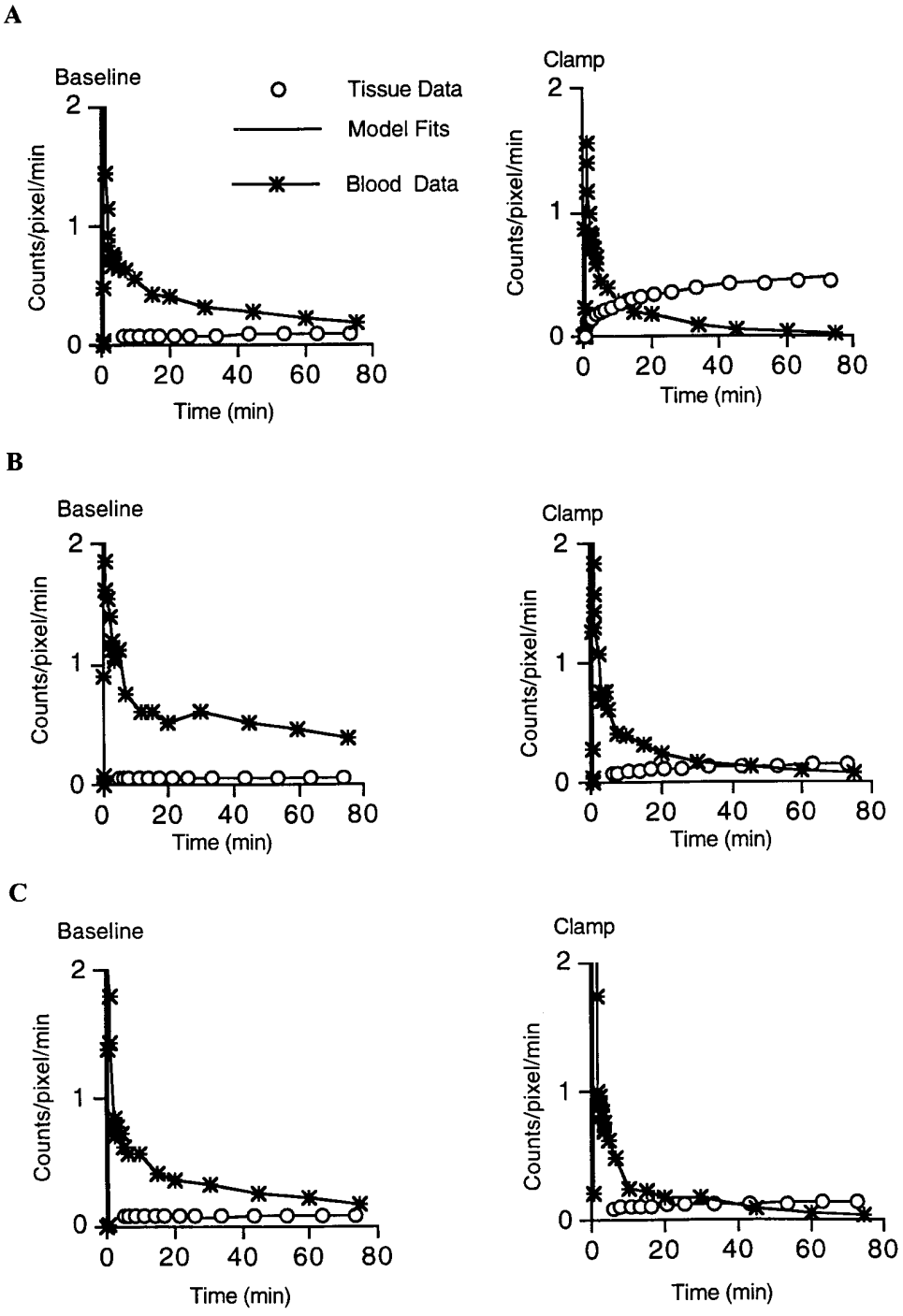

Figure 1. Representative examples of muscle tissue (o) and blood (*) FDG time-activities and 3-compartment model fits (----) for baseline (*left*) and clamp (*right*) conditions are shown in a lean volunteer (*A*), an obese nondiabetic volunteer (*B*) and a volunteer with NIDDM (*C*).

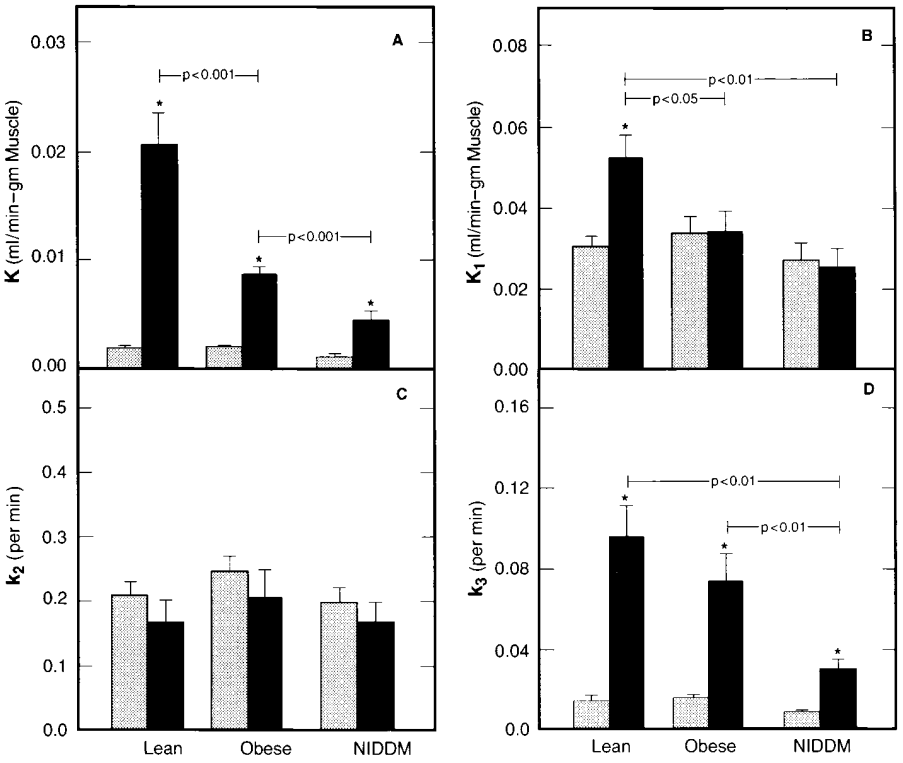

Figure 2. In *A*, data from lean and obese nondiabetic and obese NIDDM subjects during basal (*shaded bars*) and insulin-stimulated (*solid bars*) conditions are shown for ^{18}FDG clearance (K) into mid-thigh muscle; in *B*, the rate constant for transport of ^{18}FDG (K_1) is shown; in *C*, the rate constant for outward transport (k_2) of ^{18}FDG is shown; and in *D*, the rate constant for ^{18}FDG phosphorylation (k_3) during basal and insulin-stimulated conditions is shown. *Significant within-group difference comparing basal and insulin-stimulated values ($P < 0.05$). Significant group differences are indicated above the bars.

stimulated K was 10-fold greater than basal, and greater than respective values in obese ($P < 0.001$) and NIDDM subjects ($P < 0.001$). Insulin-stimulated K was also greater in obese subjects than in those with NIDDM ($P < 0.01$). Across the entire group of subjects, insulin-stimulated K was strongly correlated with systemic insulin sensitivity ($r = 0.83$, $P < 0.01$), as shown in Fig. 3. This relationship is consistent with skeletal muscle being a key determinant of systemic insulin sensitivity.

K is calculated from the rate constants K_1, k_2, and k_3, which respectively represent inward transport, outward transport and phosphorylation of FDG. Basal and insulin-stimulated values for each rate constant are shown in Fig. 2, *B–D*. There were no group differences in K_1 during basal conditions. During insulin infusion, K_1 in lean subjects was significantly greater than in obese ($P < 0.02$) or NIDDM subjects ($P < 0.001$). In lean subjects, insulin stimulated a significant increase in K_1 compared with basal values ($P < 0.001$) but had no significantly effect on K_1 in either obese or NIDDM subjects. Insulin-stimulated K_1 was not significantly different in obese and NIDDM subjects. The rate constant for outward transport of glucose, k_2, neither changed during insulin infusion (compared with basal conditions) nor differed across groups. During basal conditions, NIDDM subjects had lower k_3, the rate constant for FDG phosphorylation, than did obese ($P < 0.01$) or lean subjects ($P < 0.05$). Basal values for k_3 were similar in lean and obese subjects. Insulin-stimulated k_3 was significantly increased compared with basal for all groups ($P < 0.01$), and there was a highly significant group difference in insulin-stimulated k_3 ($P < 0.001$). Insulin-stimulated k_3 was similar in lean and obese nondiabetic subjects and greater than in subjects with NIDDM ($P < 0.01$). Across the entire group of subjects, insulin sensitivity (M) was significantly correlated with K_1 ($r = 0.57$, $P < 0.01$), and k_3 ($r = 0.60$, $P < 0.01$), and the effects of K_1 and k_3 were independently significant in multiple regression. The partial correlation between k_2 and M was not significant.

Insulin-stimulated translocation of Glut 4. The presence of Glut 4 at the sarcolemma was assessed by immunohistochemical labeling and quantitative confocal laser scanning microscopy of vastus lateralis skeletal muscle. Basal values for num-

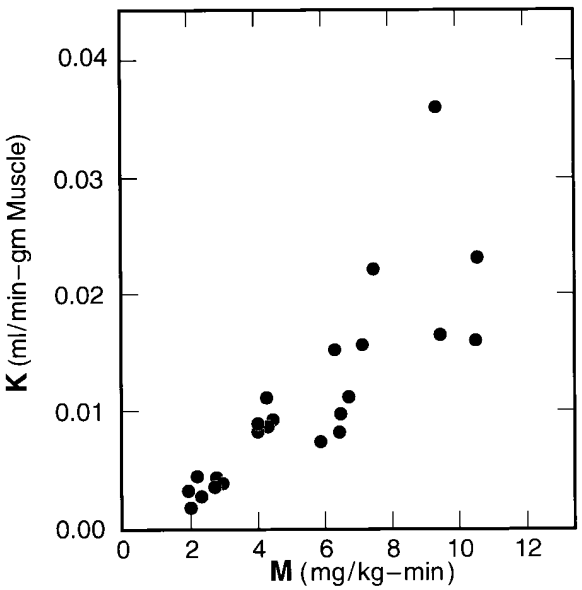

Figure 3. Insulin-stimulated rates of systemic utilization of glucose (M), in mg/kg per min, in lean and obese nondiabetic and NIDDM subjects are plotted against respective individual values for insulin-stimulated K (ml/min per gram muscle); K is the PET parameter of ^{18}FDG clearance from blood to muscle. The correlation between K and M is: $r = 0.83$, $P < 0.01$.

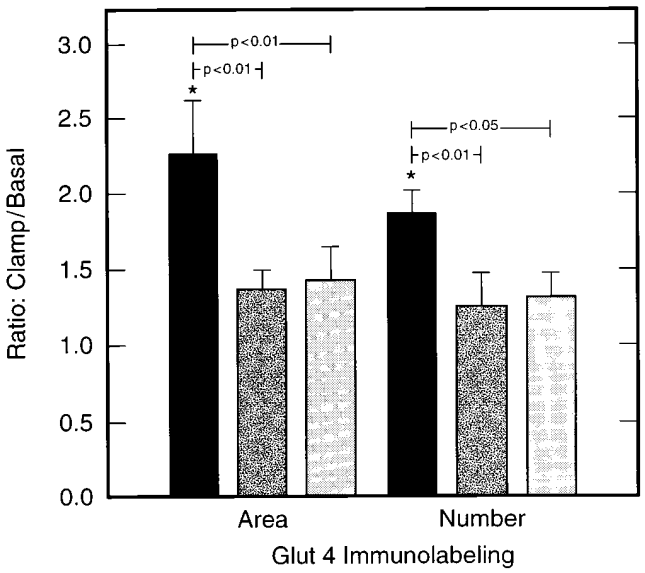

Figure 4. The ratio (insulin-stimulated to basal) for immunolabeled Glut 4 at the sarcolemma of vastus lateralis muscle is shown for lean (*solid bars*) and obese (*light shading*) nondiabetic subjects, and obese NIDDM subjects (*dark shading*). The three bars on the left represent the ratio for the area of Glut 4 label sites (μm^2) and the three bars on the right represent the ratio for numbers of Glut 4 label sites (sites per μm of sarcolemma). Imaging of immunolabeled Glut 4 was done using quantitative confocal laser scanning microscopy. Significant group differences are indicated above the bars.

ber of Glut 4 label sites were: 0.035±0.013, 0.034±0.012, and 0.034±0.010 sites per μm of sarcolemma, in L, O, and NIDDM. During insulin-stimulated conditions, these values were: 0.066±0.018, 0.047±0.014, and 0.042±0.013 sites per μm of sarcolemma, respectively. Basal values for the mean area of a Glut 4 label site were: 0.099±0.02, 0.094±0.03, and 0.092±0.02 μm^2 per μm of sarcolemma, in L, O, and NIDDM; and during insulin-stimulated conditions, these values were: 0.19±0.04. 0.16±0.04, and 0.14±0.03 μm^2 per μm of sarcolemma, respectively. Among the entire groups of subjects, insulin stimulated a significant increase in the number ($P < 0.01$) and area ($P < 0.01$) of sarcolemma labeling of Glut 4. Insulin-stimulated increases in the number of sites labeling for Glut 4 was positively correlated with the increase in area of Glut 4 label sites ($r^2 = 0.79$, $P < 0.01$). There were significant group differences in each parameter of Glut 4 labeling at the sarcolemma, as shown in Fig. 4. In lean subjects, the ratio (insulin to basal) for number of Glut 4 label sites (1.8±0.2) was greater than the ratio in obese (1.3±0.2, $P < 0.01$ vs. L) or NIDDM subjects (1.3±0.3, $P < 0.02$ vs. L), with nearly identical ratios in obese and NIDDM subjects. Similarly, the ratio for area of Glut 4 label sites was greater in lean than in either obese or NIDDM subjects (both $P < 0.01$, for both) and did not differ between obese and NIDDM subjects. Intensity of Glut 4 labeling was not affected by insulin infusion.

Skeletal muscle HK (I and II) and CS activity. Hexokinase activity in vastus lateralis muscle was not significantly different across groups. During insulin-stimulated conditions, lean, obese and NIDDM subjects had similar values for activity of HK I (0.65±0.10, 0.71±0.09, and 0.82±0.09 U/gram wet weight muscle) and for HK II (1.20±0.11, 1.22±0.07, and 1.30±0.15 U/gram wet weight muscle). Total HK activity in vastus lateralis muscle obtained during basal conditions (1.89±0.17, 1.95±0.11, and 2.06±0.10 U/gram wet weight muscle) did not differ significantly from total HK activity during insulin-stimulated conditions (1.85±0.13, 1.93±0.11, and 2.13±0.17 U/gram wet weight muscle), in L, O and NIDDM subjects respectively. Skeletal muscle CS activity was lower in NIDDM ($P < 0.05$) than in obese or lean subjects (8.58±0.85, 8.13±0.34, and 6.83±0.41 U/gram-wet weight muscle). The ratio of HK to CS enzyme activity levels, an index reflecting proportionality between glycolytic and oxidative enzyme capacities (41), was highest in NIDDM ($P < 0.01$); 0.23±0.02, 0.24±0.01, and 0.31±0.02 in L, O and NIDDM respectively. The glucose phosphorylation rate constant, k_3, was negatively correlated with the HK/CS ratio ($r = -0.46$, $P < 0.05$); the correlation between HK and k_3 was not significant ($r = -0.24$); nor was there a significant correlation between either HK I or HK II and k_3. Insulin sensitivity (M) was negatively correlated with the HK/CS ratio ($r = -0.60$, $P < 0.01$). CS activity was significantly correlated with K_1 ($r = 0.65$, $P < 0.01$), though not with k_3 ($r = 0.30$). In a multiple regression model, CS activity and Glut 4 ratio (insulin to basal) accounted for 50% of the variance in K_1, ($P < 0.001$).

Discussion

The purpose of the current study was to assess insulin regulation of glucose transport and phosphorylation in skeletal muscle to test the hypothesis that impairment contributes to insulin resistance in obesity and NIDDM. Because glucose transport is regarded as rate-limiting for insulin-stimulated glucose utilization by skeletal muscle (1, 2), impairment could have a major role in the pathogenesis of insulin resistance in NIDDM and obesity. It has, however, been technically difficult to isolate glucose transport and phosphorylation during in vivo human studies. The glucose clamp method, though widely used to measure insulin sensitivity, does not per se separate transport and phosphorylation from subsequent steps of glucose metabolism. The approach used in the current study was PET imaging of ^{18}FDG uptake into muscle. One advantage of PET is noninvasive regional imaging, but even more fundamental to the objectives of the current study is that FDG metabolism during the interval of imaging is effectively truncated following transport and phosphorylation. Therefore, the kinetics of FDG uptake reflect the proximal steps of glucose metabolism (21–24). In lean healthy volunteers, physiologic hyperinsulinemia doubled the basal rate constant for inward transport of glucose and stimulated an eightfold increase in the rate constant for glucose phosphorylation. This occurred in conjunction with a 10-fold stimulation of FDG clearance by muscle of lean volunteers, a finding similar to leg balance studies of insulin action on glucose uptake (42). In contrast to the findings in lean, healthy volunteers, PET imaging in subjects with NIDDM and obesity revealed marked insulin resistance at the step of glucose transport. In subjects with NIDDM, an additional impairment of insulin action was a blunted stimulation of the rate constant for glucose phosphorylation. Consonant with data from PET imaging on glucose transport, obese and NIDDM subjects had similar impairment of insulin regulated translocation of Glut 4 in skeletal muscle, as revealed by quantitative confocal laser scanning microscopy. These findings

support the hypothesis that impairment in glucose transport and phosphorylation have key roles in the pathogenesis of insulin resistance.

Positron emission tomography was developed approximately 40 years ago and its contemporary use is increasing because of the value of a noninvasive modality for assessing regional metabolism. To a limited extent, PET imaging has been used to examine insulin regulation of glucose metabolism in skeletal muscle. Nuutilia et al. found a strong correlation between PET measurement of insulin-stimulated uptake of FDG into skeletal muscle and systemic or forearm uptake of glucose (26–28). Of interest, these investigators estimated that the "lumped constant" for FDG, relating FDG to actual glucose uptake, is approximately one (26), suggesting minor analog effects in skeletal muscle. Rates constants for glucose transport or phosphorylation were not presented (26–28), and dynamic characterization of FDG uptake into skeletal muscle was not obtained in these studies due to PET imaging of myocardial uptake of FDG for the initial 40 min. Mossberg et al. have validated dynamic PET imaging for studies of insulin-stimulated glucose metabolism in rabbit muscle (29). PET derived rate constants for insulin-stimulated FDG metabolism in skeletal and cardiac muscle have also been reported in a few human studies. During insulin infusion studies, Selberg et al. found that individuals with cirrhosis had reduced K_1, increased k_2, and no difference in k_3 in skeletal muscle as compared with values in healthy volunteers (30). In a study of individuals with myotonic dystrophy, correlation was found between k_3 and the length of genetic mutation encoding a protein kinase involved in enzyme activation (31). The use of PET imaging in NIDDM is quite limited. Insulin-stimulated FDG uptake in skeletal muscle was equivalent in hyperglycemic NIDDM and euglycemic nondiabetic subjects (43), findings consistent with hyperglycemic compensation of insulin resistance in NIDDM (44). Insulin-stimulated FDG clearance in myocardium is reduced in NIDDM (45). The current study is the first to use PET imaging to examine insulin-stimulated FDG uptake into skeletal muscle in NIDDM subjects during steady-state euglycemic conditions, and the first study which presents rate constants for glucose transport and phosphorylation in skeletal muscle of insulin sensitive and resistant subjects.

Taking into account in vitro studies, there are extensive data which implicate perturbations of glucose transport in the pathogenesis of insulin resistance in NIDDM and obesity (2, 9, 46–48). Garvey et al. reported reduced number and activity of glucose transporters in primary cultures of adipocytes from obese and NIDDM subjects (46). Dohm and colleagues, in fresh incubations of human rectus abdominous muscle, found severe impairment of insulin-stimulated glucose transport in NIDDM and noted that this defect was of similar magnitude to that of individuals with marked obesity (47). Intriguingly, in the current study, moderately obese nondiabetic and NIDDM subjects had similar impairment of insulin-stimulated glucose transport. During in vivo studies using ^{13}C-NMR, Rothman et al. detected lower [G-6-P] in gastrocnemius muscle in subjects with NIDDM during insulin-stimulated conditions (17). This finding is indicative of either impaired transport or phosphorylation of glucose, but this method does not distinguish between these possibilities. Bonnadonna et al., using a novel isotope and limb balance approach, found defects in both transport and phosphorylation in NIDDM (19, 20). In those studies (19, 20), insulin-stimulated glucose transport was reduced by approximately one-half in NIDDM. This is similar to the approximately 50% reduction in the rate constant for inward transport of glucose in NIDDM observed in the current study. The current findings and those of Bonnadonna et al. (20), are further congruent in that NIDDM is found to adversely affect insulin-stimulated glucose phosphorylation.

The current study also delineates a mechanism which could account for impaired glucose transport in obesity and NIDDM. Collateral to in vivo PET imaging studies, ex vivo analysis of insulin-regulated Glut 4 translocation in skeletal muscle was assessed using confocal laser scanning microscopy. High resolution structural microscopy has previously been used to study insulin-regulated Glut 4 translocation in muscle (37, 49). In the current study, obesity and NIDDM were found to adversely affect this crucial step of insulin-stimulated glucose transport. In lean healthy subjects, insulin stimulated nearly a two-fold increase in the number and area of sites labeling for Glut 4 along the sarcolemma. This is implicit evidence of insulin-stimulated translocation of Glut 4 and quantitatively similar to the findings of Guma et al. (50). That study, the first quantitative data on insulin-regulated Glut 4 translocation in human skeletal muscle, reported a 1.6-fold insulin-stimulated increment in Glut 4 within plasma membranes based on sub-cellular fractionation methods (50). The important new finding in the current study is that obese and NIDDM subjects have blunted, though not absent, insulin-stimulation of Glut 4 translocation. This similarity between obese NIDDM and obese nondiabetics for Glut 4 translocation echoes the pattern found with PET imaging. Together, these data buttress the concept that a crucial element of insulin-resistance in obesity and NIDDM is impaired Glut 4 translocation and function. Since the NIDDM subjects in the current study were moderately obese, as are most patients with NIDDM, it is tempting to speculate that obesity may be a key factor mediating insulin-resistance of glucose transport (47–49).

Skeletal muscle was also analyzed for hexokinase activity and activities for both HK I and II were similar lean, obese and NIDDM subjects. Phosphorylation of glucose, mediated by hexokinase, is regarded as functionally coupled to transport (51–53). The phosphorylation of glucose is essential to transport because this traps glucose and maintains a concentration gradient across the cell surface for free glucose. In the current study, approximately two-thirds of skeletal muscle hexokinase activity was attributable to hexokinase II, which is consistent with known patterns of expression in muscle (52). In a recent study, similar HK activity in muscle of nondiabetic and NIDDM subjects was also observed (13). Katz et al. also found that insulin infusion did not acutely stimulate HK activity in healthy volunteers, and did not affect HK distribution between cytosolic and mitochondrial fraction (54). In the current study, muscle HK activity, though consistent with prior studies, does not account for insulin resistance of glucose phosphorylation in NIDDM, as detected by PET imaging. However, NIDDM was associated with alteration of the proportionality between HK and CS activity levels, and this parameter, the HK/CS ratio, was negatively correlated with k_3, the rate constant for glucose phosphorylation. This enzyme ratio was also negatively correlated with insulin sensitivity, and is consistent with prior observations that an elevated ratio of glycolytic to oxidative enzyme capacities is a biochemical characteristic of insulin resistant skeletal muscle (55). These findings suggest that mismatching between HK and CS activities, the latter a marker of mito-

chondrial content in skeletal muscle, is associated with insulin-resistance of glucose phosphorylation. The correlation between skeletal muscle CS activity and the rate-constant for inward transport of glucose is also consistent with the concept that muscle fibers with enhanced oxidative capacity manifest increased insulin sensitivity (56).

In the current study, dynamic PET imaging of FDG uptake into skeletal muscle was analyzed using a three-compartment model to mathematically derive rate constants for transport (inward and outward) and phosphorylation of glucose. This modeling of PET data was originally developed and then validated for brain (23), and later validated for myocardium (24). It is important to emphasize that this model does not contain coefficients specific for brain metabolism or intrinsically biased toward the biochemistry of other organ systems. In the current study, application of this model during basal and insulin-stimulated conditions revealed clear-cut effects of insulin-stimulation, distinct differences between groups known to differ in insulin sensitivity, and strong correlation between individual variation in PET parameters and independently determined insulin sensitivity. Furthermore, steady-state insulin-stimulated conditions of equivalent arterial glucose and insulin were achieved which is stipulated in the assumptions behind the application of this model and the uniformity of these conditions enhances comparisons across groups. It seems unlikely that observed group differences are due to group differences in analog effects of FDG. In the first place, there were no significant differences across groups during basal conditions, but only during steady-state insulin stimulation. Further, it seems unlikely that analog effect would fundamentally differ in obesity or NIDDM since neither the primary structure nor the content of Glut 4 and HK II are abnormal in a large majority of patients with NIDDM (4–7, 10–12). However; empiric determination of analog effects in obesity and NIDDM have not been performed.

Differences between lean, obese and NIDDM subjects for the rate constant of inward transport of glucose could reflect group differences in insulin regulation of blood flow to skeletal muscle. The rate constant for inward transport of glucose describes the efficiency of glucose movement from blood to tissue and insulin resistance in the stimulation of blood flow (57), or factors such as reduced capillary density (58), could potentially influence the rate constant for inward transport of glucose. Nevertheless, the findings in the current study of impaired Glut 4 translocation indicate that altered cellular mechanisms have an important role in the insulin resistance of glucose transport.

In summary, in vivo PET imaging of insulin-stimulated FDG uptake into skeletal muscle indicates that glucose transport is impaired in obesity and NIDDM. The insulin resistance of NIDDM is also characterized by an additional impairment in glucose phosphorylation. Immunohistochemical labeling of Glut 4 in muscle and quantitative confocal laser scanning microscopy reveal that obesity and NIDDM share a similar defect in insulin-regulated Glut 4 translocation and that this may be the mechanism accounting for functional perturbation of insulin-regulated glucose transport. Though hexokinase activity in muscle is not deficient in NIDDM, reduced efficiency of glucose phosphorylation in NIDDM is associated with an increased ratio of HK to citrate synthase activity, suggesting a poor coupling between HK activity and capacity for production of ATP via oxidative substrate metabolism in NIDDM. We conclude that insulin-stimulated glucose transport is impaired in obesity and NIDDM and that additional pertubation of glucose phosphorylation contributes to the pathogenesis of insulin resistance in NIDDM.

Acknowledgments

We are grateful to our research volunteers, and for the nursing, dietary, and technician staff support at the General Clinical Research Center, the Positron Emission Tomography Center, and the Structural Biology Imaging Center at the University of Pittsburgh. We would also like to acknowledge the technical expertise of Yves Gélinas, of Laval University.

These studies were supported by the University of Pittsburgh General Clinical Research Center (5MO1RR00056), the University of Pittsburgh Obesity and Nutrition Research Center (1P30DK46204), a Veterans Affairs Merit Award, the Natural Sciences and Engineering Council of Canada, and the Font de la Recherche en Sante du Quebec (FRSQ).

References

1. Katz, A., B.L. Nyomba, and C. Bogardus. 1988. No accumulation of glucose in human skeletal muscle during euglycemic hyperinsulinemia. *Am. J. Physiol.* (*Endocrinol. Metab.*) 255:E942–E945.

2. Ziel, F.H., N. Venkatesan, and M.B. Davidson. 1988. Glucose transport is rate limiting for skeletal muscle glucose metabolism in normal and STZ-induced diabetic rats. *Diabetes.* 37:885–890.

3. Kahn, B. 1992. Facilitative glucose transporters: regulatory mechanisms and dysregulation in diabetes. *J. Clin. Invest.* 89:1367–1374.

4. Pederson, O., J.F. Bak, P.H. Andersen, S. Lund, D.E. Moller, J.S. Flier, and B.B. Kahn. 1990. Evidence against altered expression of GLUT1 or GLUT4 in skeletal muscle of patients with obesity or NIDDM. *Diabetes.* 39:865–870.

5. Garvey, W.T., L. Maianu, J.A. Hancock, A.M. Golichowski, and A. Baron. 1992. Gene expression of GLUT4 in skeletal muscle from insulin-resistant patients with obesity, IGT, GDM, and NIDDM. *Diabetes.* 41:465–475.

6. Baroni, M.G., R.S. Oelbaum, P. Pozzilli, J. Stocks, S.-R. Li, V. Fiore, and D.J. Galton. 1992. Polymorphisms at the GLUT1 (HepG2) and GLUT4 (muscle/adipocyte) glucose transporter genes and non–insulin-dependent diabetes mellitus (NIDDM). *Hum Genet.* 88:557–561.

7. Choi, W.-H., S. O'Rahilly, J.B. Buse, A. Rees, R. Morgan, J. Flies, and D.E. Moller. 1991. Molecular scanning of insulin-responsive glucose transporter (GLUT4) gene in NIDDM subjects. *Diabetes.* 40:1712–1718.

8. Bell, G.I., T. Kayano, J.B. Buse, C.F. Burant, J. Takeda, D. Lin, H. Fukumoto, and S. Seino. 1990. Molecular biology of mammalian glucose transporters. *Diabetes Care.* 13(3):198–208.

9. Klip, A., and M.R. Paquet. 1990. Glucose transport and glucose transporters in muscle and their metabolic regulation. *Diabetes Care.* 13:228–243.

10. Laakso, M., M. Malkki, and S.S. Deeb. 1995. Amino acid substitutions in hexokinase II among patients with NIDDM. *Diabetes.* 44:330–334.

11. Vidal-Puig, A., R.L. Printz, I.M. Stratton, D.K. Granner, and D.E. Moller. 1995. Analysis of the hexokinase II gene in subjects with insulin resistance and NIDDM and detection of a $Gln^{142} \rightarrow$ His substitution. *Diabetes.* 44:340–346.

12. Echwald, S.M., C. Bjorbaek, T. Hansen, J.O. Clausen, H. Vestergaard, J.R. Zierath, R. Printz, D.K. Granner, and O. Pederson. 1995. Identification of four amino acid substitutions in hexokinase II and studies of relationships to NIDDM, glucose effectiveness, and insulin sensitivity. *Diabetes.* 44:347–353.

13. Kelley, D.E., and J.-A. Simoneau. 1994. Impaired free fatty acid utilization by skeletal muscle in non–insulin dependent diabetes mellitus. *J. Clin. Invest.* 94:2349–2356.

14. DeFronzo, R.A., J.D. Tobin, and R. Andres. 1979. Glucose clamp technique: a method of quantifying insulin secretion and resistance. *Am. J. Physiol.* 237:E214–E223.

15. Butler, P.C., E.J. Kryshak, M. Marsh, and R.A. Rizza. 1990. Effect of insulin on oxidation of intracellularly and extracellularly derived glucose in patients with NIDDM: evidence for primary defect in glucose transport and/or phosphorylation but not oxidation. *Diabetes.* 39:1371–1380.

16. Shulman, G., D. Rothman, T. Jue, and P. Stein. 1990. Quantitation of muscle glycogen synthesis in normal subjects with NIDDM by ^{13}C nuclear magnetic resonance spectroscopy. *N. Engl. J. Med.* 322:223–228.

17. Rothman, D.L., R.G. Shulman, and G.I. Shulman. 1992. ^{31}P nuclear magnetic resonance measurements of muscle glucose-6-phosphate evidence for reduced insulin-dependent muscle glucose transport or phosphorylation activity in non-insulin-dependent diabetes mellitus. *J. Clin. Invest.* 89:1069–1075.

18. Bonadonna, R.C., M.P. Saccomani, L. Seely, K.S. Zych, E. Ferrannini, C. Cobelli, and R.A. DeFronzo. 1993. Glucose transport in human skeletal

muscle. The in vivo response to insulin. *Diabetes.* 42:191–198.

19. Bonadonna, R.C., S. Del Prato, M.P. Saccomani, E. Bonora, G. Gulli, E. Ferrannini, D. Bier, C. Cobelli, and R.A. DeFronzo. 1993. Transmembrane glucose transport in skeletal muscle of patients with non–insulin-dependent diabetes. *J. Clin. Invest*. 92:486–494.

20. Bonnadonna, R.C., M.P. Saccomani, S. Del Prato, E. Bonora, D. Bier, C. Cobelli, and R.A. DeFronzo. 1994. Mechanisms of normalization of muscle glucose uptake by hyperglycemia in NIDDM. *Diabetes* 43:72A.

21. Hansen, P.A., E.A. Gulve, and J.O. Holloszy. 1994. Suitability of 2-deoxyglucose for in vitro measurement of glucose transport activity in skeletal muscle. *J. Appl. Physiol.* 76(2):979–985.

22. Fowler, J.S., and A.P. Wolf. 1986. 2-Deoxy-2-[^{18}F]Fluoro-D-Glucose for Metabolic Studies: Current Status. *Appl. Radiat. Isot.* 37:663–668.

23. Phelps, M.E., S.C. Huang, E.J. Hoffman, C. Selin, L. Sokoloff, and D.E. Uhl. 1979. Tomographic Measurement of local cerebral glucose metabolic rate in humans with (F-18) 2-Fluoro-2-deoxy-D-glucose: Validation of method. *Ann. Neurol.* 6:371–388.

24. Huang, S.C., B.A. Williams, J.R. Barrio, J. Krivokapic, C. Nissenson, E.J. Hoffman, and M.E. Phelps. 1987. Measurement of glucose and 2-deoxy-2 [^{18}F]fluoro-D-glucose transport and phosphorylation rates in myocardium using dual-tracer kinetic experiments. *FEBS Lett.* 216:128–132.

25. Sokoloff, L., M. Reivich, C. Kennedy, M.S. DesRosiers, C.S. Pottak, K.D. Pettigrew, O. Sakurada, and M. Shinohara. 1977. The [14-C] deoxyglucose method of local cerebral glucose utilization: Theory, procedure, and normal values in the conscious and anesthetized albino rat. *J. Neurochem.* 28:897–916.

26. Nuutila, P., V.A. Kinisto, J. Knwuti, U. Ruotsalainen, M. Teräs, M. Haaparanta, O. Solin, and H. Yki-Jarvinen. 1992. Glucose-free fatty acid cycle operates in human heart and skeletal muscle in vivo. *J. Clin. Invest.* 89:1767–1774.

27. Nuutila, P., M.J. Knuuti, M. Mäki, H. Laine, U. Ruotsalainen, M. Teräa, M. Haaparanta, O. Solin, and H. Yki-Jarvinen. 1995. Gender and insulin sensitivity in the heart and in skeletal muscles. *Diabetes.* 44:31–36.

28. Nuutila, P., M. Maki, H. Laine, M.J. Knvuti, U. Ruotsalainen, M. Luotolahti, M. Hoaparanta, O. Solin, A. Jula, V.A. Kaivisto, L.M. Voijo-Pulkki, and H. Jki-Jarvinen. 1995. Insulin action on heart and skeletal muscle glucose uptake in essential hypertension. *J. Clin. Invest.* 96:1003–1009.

29. Mossberg, K.A., and H. Taegtmeyer. 1992. Time course of skeletal muscle glucose uptake during euglycemic hyperinsulinemia in the anesthetized rabbit: afluorine-18-2-Deoxy-2-fluoro-D-glucose Study. *J. Nucl. Med.* 33:1523–1529.

30. Selberg, O., W. Burchert, J. v.d.Hoff, G.J. Meyer, H. Hundeshagen, E. Radoch, H.-J. Balks, and M. J. Muller. 1993. Insulin resistance in liver cirrhosis: positron emission tomography scan analysis of skeletal muscle glucose metabolism. *J. Clin. Invest.* 91:1897–1902.

31. Annane, D., D. Duboc, B. Mazoyer, P. Merlet, M. Fiorelli, B. Eymard, H. Radvanyi, C. Junien, M. Fardeau, P. Gajdos, F. Guerin, and A. Syrota. 1994. Correlation between decreased myocardial glucose phosphorylation and the dna mutation size in myotonic dystrophy. *Circulation.* 90:2629–2634.

32. National Diabetes Data Group. 1979. Classification and diagnosis of diabetes mellitus and other categories of glucose intolerance. *Diabetes.* 28:1039–1057.

33. Evans, W., S. Phinney, and V. Young. 1982. Suction applied to a muscle biopsy maximizes sample size. *Med. Sci. Sports. Exer.* 14:101–102.

34. Finegood, D., R. Bergman, and M. Vranic. 1988. Modeling error and apparent isotope discrimination confound estimation of endogenous glucose production during euglycemic glucose clamps. *Diabetes.* 37:1025–1034.

35. Hamacher, K., H.H. Coenen, and G. Stocklin. 1986. Efficient stereospecific synthesis of no carrier added 2-[^{18}F]fluoro-2-deoxy-D-glucose using aminopolyether supported nucleophilic substitution. *J. Nucl. Med.* 27:235.

36. Revich, M., A. Alavi, A. Wolf, J. Fowler, J. Russell, C. Aractt, R.R. MacGregor, C.Y. Shiru, H. Atkins, A. Anand, R. Dann, and J.H. Greenberg. 1985. Glucose metabolic rate kinetic model parameter determination in humans: the lumped constants and rate constant for [18F] Fluorodeoxyglucose and [11C]Deoxyglucose. *J. Cereb. Blood Flow Metab.* 9:179–192.

37. Piper, R., L.J. Hess, and D.E. James. 1991. Differential sorting of two glucose transporters in insulin-sensitive cells. *Am. J. Physiol.* 260 (*Cell Physiol.* 29):C570–C580.

38. Howald, H., D. Pette, J.-A. Simoneau, A. Uber, H. Hoppler, and P. Cerretelli. 1990. III. Effects of chronic hypoxia on muscle enzymes activities. *Int. J. Sports Med*. 11:S10–S14.

39. Katzen, H.M., D.D. Soderman, and C.E. Wiley. 1970. Multiple forms of hexokinase. Activities associated with subcellular particulate and soluble fractions of normal and streptozotocin diabetic rat tissues. *J. Biol. Chem*. 245:4081–4096.

40. Colberg, S.R., J.-A. Simoneau, L.F. Thaete, and D.E. Kelley. 1995. Skeletal muscle utilization of free fatty acids in women with visceral obesity. *J. Clin. Invest.* 95:1846–1853.

41. Pette, D., and R.S. Staron. 1990. Cellular and molecular diversities of mammalian skeletal muscle fibers. *Rev. Physiol. Biochem. Pharmacol.* 116:1–76.

42. Kelley, D.E., J.P. Reilly, T. Veneman, and L.J. Mandarino. 1990. Effects of insulin on skeletal muscle glucose storage, oxidation, and glycolysis in humans. *Am. J. Physiol.* 258 (*Endocrinol. Metab.* 21): E923–E929.

43. Voipio-Pulkki, L.-M., and P. Nuutilia. 1993. Heart and skeletal muscle glucose disposal in type 2 diabetic patients as determined by positron emission tomography. *J. Nucl. Med.* 34:2064–2067.

44. Kelley, D.E., and L.J. Mandarino. 1990. Hyperglycemia normalizes insulin-stimulated skeletal muscle glucose oxidation and storage in noninsulin-dependent diabetes mellitus. *J. Clin. Invest.* 86:1999–2007.

45. Ohtake, T., I. Yokoyama, T. Wantanabe, T. Monose, J. Serezawa, J. Nishikawa, and Y. Sasaki. 1995. Myocardial glucose metabolism in noninsulin-dependent diabetes mellitus patients evaluated by FDG-PET. *J. Nucl. Med.* 36: 456–463.

46. Garvey, T.W., T.P. Hueckstead, S. Matthaei, and J.M. Olefsky. 1988. Role of glucose transporters in the cellular insulin resistance of Type II non–insulin-dependent diabetes mellitus. *J. Clin. Invest.* 81: 1528–1536.

47. Dohm, G.L., E.B. Tapscott, W.J. Pories, D.J. Dobbs, E.G. Flickinger, D. Meelheim, T. Fushiki, S.M. Atkinson, C. Elton, and J.F. Caro. 1988. An in vitro human muscle preparation suitable for metabolic studies decreased insulin stimulation of glucose transport in muscle from morbidly obese and diabetic subjects. *J. Clin. Invest.* 82:486–494.

48. Sherman, W.M., A.L. Katz, C.L. Cutler, R.T. Withers, and J.L. Ivy. 1988. Glucose transport: locus of muscle insulin resistance in obese Zucker rats. *Am. J. Physiol.* 255 (*Endocrinol. Metab. Physiol.*):E374–E382.

49. Rodnick, K.J., J.W. Slot, D.R. Studelska, D.E. Hanpeter, L.J. Robinson, H.J. Geuze, and D.E. James. 1992. Immunocytochemical and biochemical studies of GLUT4 in rat skeletal muscle. *J. Biol. Chem.* 267(9):6278–6285.

50. Guma, A., J.R. Zierath, H. Wallberg-Henriksson, and A. Klip. 1995. Insulin induces translocation of GLUT-4 glucose transporters in human skeletal muscle. *Am. J. Physiol.* 268 (*Endocrinol. Metab.* 31):E613–E622.

51. Kong, X., J. Manchester, S. Salmons, and J.C. Lawrence, Jr. 1994. Glucose transporters in single skeletal muscle fibers. *J. Biol. Chem.* 17:12963–12967.

52. Postic, C., A. Leturque, R.L. Printz, P. Maulard, M. Loiseau, D.K. Grannes, and J. Girard. 1994. Development and regulation of glucose transporter and hexokinase expression in rat. *Am. J. Physiol.* 266 (*Endocrinol. Metab.* 29): E548–E559.

53. Hofmann, S., and D. Pette. 1994. Low-frequency stimulation of rat fast-twitch muscle enhances the expression of hexokinase II and both the translocation and expression of glucose transporter 4 (Glut-4). *Eur. J. Biochem.* 219:307–315.

54. Katz, A., and I. Raz. 1994. Hexokinase kinetics in human skeletal muscle after hyperinsulinemia, hyperglycemia and hyperepinephrinaemia. *Acta Physiol. Scand.* 151:527–530.

55. Simoneau, J.-A., S.R. Colberg, F.L. Thaete, and D.E. Kelley. 1995. Skeletal muscle glycolytic and oxidative enzyme capacities are determinants of insulin sensitivity and muscle composition in obese women. *FASEB J.* 9:273–278.

56. Hickey, M.S., M.D. Weidner, K.E. Gavigan, D. Zheng, G.L. Tyndall, and J.A. Houmard. 1995. The insulin action-fiber type relationship in humans is muscle group specific. *Am. J. Physiol.* 269 (*Endocrinol. Metab.* 32):E150–154.

57. Laakso, M., S.V. Edelman, G. Brechtel, and A.D. Baron. 1990. Decreased effect of insulin to stimulate skeletal muscle blood flow in obese man. A novel mechanism for insulin resistance. *J. Clin. Invest.* 85:1844–1852.

58. Lillioja, S., A. Young, C. Cutler, J. Ivy, W. Abbot, J. Zawadzki, H. Yki-Jarvinen, L. Christin, T. Secomb, and C. Bogardus. 1987. Skeletal muscle capillary density and fiber type are possible determinants of in vivo insulin resistance in man. *J. Clin. Invest.* 80:415–424.